Publ. Astron. Inst. ASCR 93, 21 – 28 (2005)

59 Cyg – A second Be binary with a hot, compact companion

M. Maintz[1], T. Rivinius[1], O. Stahl[1], S. Štefl[2,3], I. Appenzeller[1]

[1] *Landessternwarte, Königstuhl 12, D-69117, Heidelberg, Germany; mmaintz@lsw.uni-heidelberg.de, triviniu@lsw.uni-heidelberg.de, ostahl@lsw.uni-heidelberg.de, iappenze@lsw.uni-heidelberg.de*
[2] *Astronomical Institute, Academy of Sciences, CZ-251 65 Ondřejov, Czech Republic; sstefl@asu.cas.cz*
[3] *European Southern Observatory, Casilla 19001, Santiago 19, Chile; sstefl@eso.org*

The Be star 59 Cyg was directly confirmed to be an evolved Be binary with a sdO companion (Be + sdO) by a weak HeII 4686 absorption. Orbital elements and stellar masses were determined. The orbital period was found to be 28.192 ±0.004 d with a slightly eccentric orbit of $e = 0.11 \pm 0.005$. The mass of the secondary is located in the range between 1.56 and 2.3 $M_\odot$. Thus, 59 Cyg most likely resembles the well known Be + sdO binary ϕ Per in an earlier stage. Characteristic features for Be binaries with sdO or white dwarf companions were identified. They can be used for an easier identification of further evolved Be binaries or candidate systems.

Keywords: 59 Cyg – Be + sdO binaries – evolved binaries – ϕ Per

1 Introduction

Be stars, short for B emission line stars, are stars of spectral type B and luminosity class III, IV, and V which have or once had one or more Balmer lines in emission (Jaschek et al. 1981). About 10 to 20% of all B-type stars in the Milky Way belong to this group (Maeder et al. 1999). The emission arises in a gaseous circumstellar disc excited by UV radiation of the Be star. With rotation velocities of 70% (Slettebak 1982) maybe up to 100% (Owocki 2004) of their critical limit they belong to the most rapid rotators.

It is still not clear how Be stars form and why they rotate so rapidly. Maybe they are born as rapid rotators and can avoid spin-down during their evolution or they spin up due to core contraction when the hydrogen inside the core is exhausted. Another scenario is close binary evolution. Model calculations show that Roche-lobe overflow of the original primary can spin-up and rejuvenate the original secondary (Pols et al. 1991; Vanbeveren et al. 1998). After mass and angular momentum transfer are completed the original secondary has developed into a fast rotating Be star. It is the new primary of the evolved binary. Between 5% to 20% (Van Bever and Vanbeveren 1997), up to 50% (Pols et al. 1991) of all Be stars could have formed this way. Therefore, Be binaries are expected to represent post mass exchange binaries including a Be primary and an evolved companion.

Following Van Bever and Vanbeveren (1997) and Raguzova (2001) roughly 20% of all evolved Be binaries could have a sdO companion (Be + sdO), about 70% a white dwarf (Be + WD), and only 10% a neutron star (Be /X-ray) . According to Pols et al. (1991) more than 80% of all Be binaries should be Be + sdO binaries, less than 20% should have a white dwarf companion, and only a few % a neutron star. In contrast to these predictions only one Be + sdO binary, ϕ Per, is identified (Poeckert 1981), no single Be + WD binary is known, but more than 60 Be /X-ray binaries were found. The question is weather the predictions and, thus, the scenario of close binary evolution are wrong or if the missing Be + sdO and Be + WD binaries are not observed yet.

2 Observations

Most of the 59 Cyg spectra available to this study were obtained with the fibre-linked echelle spectrograph Flash (Mandel 1988, 1994) and its upgrade Heros (Kaufer 1996, 1998). The observing runs are listed in Tab. 1. Flash covers a spectral range of about 4000 – 6700 Å. By adding a second optical system Flash became Heros. The wavelength range was extended from roughly 3450 – 5600 Å (blue channel) to about 5800 – 8650 Å (red channel).

Data reduction was carried out using a Midas

Table I. Observing campaigns with the HEROS / FLASH spectrograph during which spectra of 59 Cyg were obtained (LSW: Landessternwarte; DSAZ: German-Spanish Astronomical Center; USM: Universitätssternwarte München).

Observing campaign	Observatory	Telescope	Instrument	Spectra
1990	LSW Heidelberg, Germany	Waltz 72 cm	FLASH	10
1997 Aug. – 1998 Feb.	LSW Heidelberg, Germany	Waltz 72 cm	HEROS	1
1998 July – Oct.	Calar Alto, DSAZ, Spain	1.23 m	HEROS	38
2000 May – July	Wendelstein, USM, Germany	60 cm	FLASH	13
2000 Aug. – 2001 Oct.	Ondřejov Obs., Czech Republic	2 m	FL. / HER.	4 / 39
2002 March – Oct.	Ondřejov Obs., Czech Republic	2 m	HEROS	11

package for the reduction of echelle spectra which is modified and adapted to HEROS data (Stahl et al. 1995). The long-term observations with the same instrument yielded a homogeneous data set. The large wavelength range of the spectra allowed for simultaneous investigation of several lines of different ions.

3 The Be + sdO binary 59 Cyg

The Be star 59 Cyg (HD 200120, HR 8047; B1–1.5Ve) is a rapid rotator with $v \sin i = 450$ km/s (Hutchings and Stoeckley 1977; Harmanec et al. 2002). It is the brightest component of a multiple stellar system that belongs to the Cyg OB7 association. Its optical spectrum is characterized by very broad lines and strong line emission. Most of the absorption lines show emission components. Broad double-peaked emission lines are visible throughout the observed spectral range.

3.1 Orbital period

Four photospheric absorption lines are nearly free of emission and, thus, suitable for radial velocity measurements. These are the helium lines HeI 4009, 4026, 4144, and 4471. They represent the motion of the Be primary. Radial velocities were determined by standard cross-correlation. For each of the helium lines a separate measurement was carried out. The whole profiles were used. As a template the average spectrum of all corresponding individual line profiles was taken. A time series analysis was applied to each set of radial velocity data separately to search for the orbital period of the binary. The analysis-of-variance method, AOV, (Schwarzenberg-Czerny 1989) and the method from Scargle (1982) to compute periodogrammes for unevenly distributed data were used. Both methods yielded the same result.

Table II. Number of spectra for the helium absorption lines of 59 Cyg, suitable for radial velocity measurements, per year and in total.

Year	HeI 4009	HeI 4026	HeI 4144	HeI 4471
1990	–	–	8	9
1997	1	1	1	1
1998	24	34	22	34
2000	21	21	19	35
2001	5	9	5	10
2002	1	2	–	2
Total	52	67	55	91

Only for HeI 4471 one significant period was found. This is not too surprising, since the numbers of suitable spectra for each of the four helium lines differ quite much (Tab. 2). The orbital period determined for 59 Cyg is $\mathcal{P} = 28.192 \pm 0.004$ d (Tab. 3). The radial velocities of HeI 4026 and HeI 4144 are sorted well with this period. HeI 4009 may follow that period, too. The data are well spread across the orbital phase, but the variations of the radial velocities are very small. It is not clear why this line does not resemble the behaviour of the other three lines.

Based on the period of 28.192 d dynamical spectra were calculated for several absorption lines of different ions. For that purpose the single profiles of a spectral line were sorted into 20 phase bins which cover an entire orbital cycle. All spectra within one bin were averaged. The averaged line profiles were plotted bin by bin into a two-dimensional frame using velocity as abscissa and phase as ordinate. The greyscale represents the local intensities. Phase 0.0 corresponds to the orbital phase when both components of the binary have reached zero radial velocity and the secondary is in front of the primary. The absorption cores of HeI 4471 (Fig. 1, left), 4144, 4026, the Balmer lines Hβ, Hγ, Hδ, and of HeI 4713 and HeI 3820 move with a velocity amplitude between 20 to 30 km/s and show the motion of the Be star clearly. Also the ultraviolet wind absorption line CIV 1548 follows the motion of the primary.

3.2 HeII 4686

The individual line profiles and the averaged spectrum do not show clear indications for a hot companion. Dynamical spectra which are more sensitive to very small variations were computed for HeII and multiple ionized metal lines. These spectral lines are characteristic for O-type star. The single line pro-

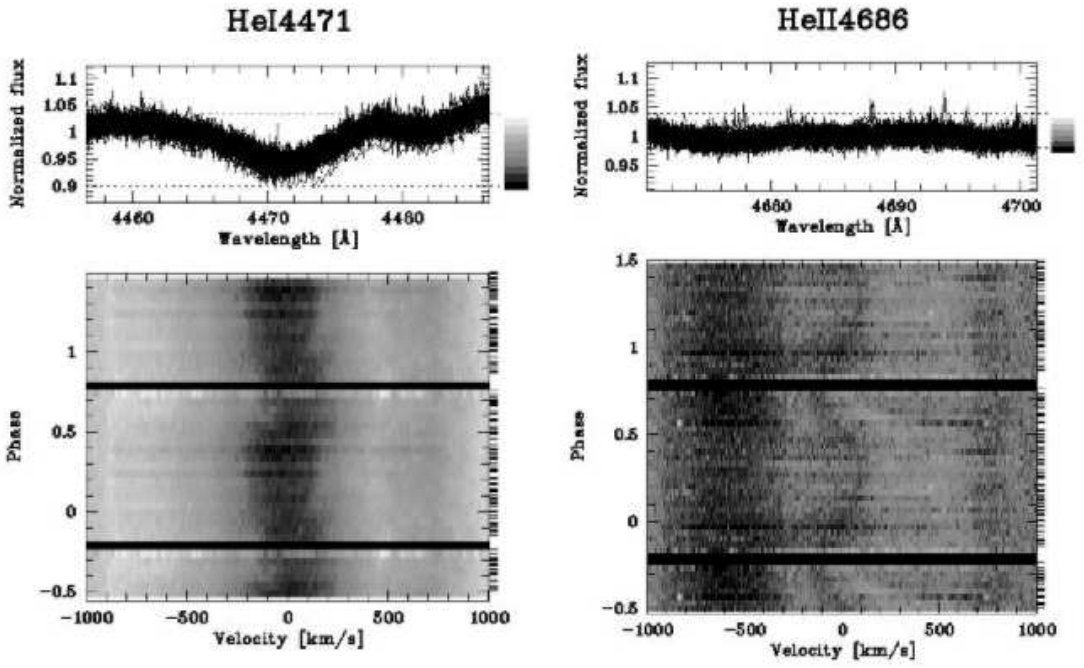

Figure 1: Dynamical spectra of the photospheric absorption lines HeI 4471 (left) and HeII 4686 (right) of the binary components of 59 Cyg. HeI 4471 moves with a velocity amplitude between 20 to 30 km/s and shows the orbital motion of the primary. HeII 4686 moves in anti-phase to the Be star with a velocity amplitude of about ±100 km/s and represents the hot, compact sdO companion.

files were sorted into 30 phase bins. In the range of HeII 4686 (Fig. 1, right) and HeII 1640 weak absorption features are clearly detectable. They are very narrow and move in anti-phase to the Be primary with a velocity amplitude of roughly ±100 km/s. For comparison the motion of the Be star is represented by the broad absorption core in the dynamical spectrum of HeI 4471 (Fig. 1, left). The absorption feature in the dynamical spectrum of HeII 4686 is very clear and can easily be traced. In contrast to HeII 1640, even early B-type stars do not show any HeII 4686 contribution. This spectral line must originate in the photosphere of the seconda ry. It constitutes a direct evidence for a hot, compact companion, and, hence, for 59 Cyg to be a Be + sdO binary system.

3.3 Stellar and orbital elements

Radial velocities were determined for the secondary component by measuring the position of the absorption core of the HeII 4686 line in each phase bin of the dynamical spectrum. Three measurements were carried out interactively with the graphical curser and averaged to get the final data set. This allowed for investigation of radial velocity curves of both binary components and for derivation not only of orbital, but also of stellar parameters (Tab. 3).

It turned out that the binary system is slightly eccentric with an eccentricity value of $e = 0.11 \pm 0.005$. One of the most interesting results is that the mass of the secondary, M_2, lies between 1.56 and 2.3 $M_\odot$ and, thus, above the Chandrasekhar limit of 1.4 $M_\odot$. This finding suggests that 59 Cyg represents an earlier stage of ϕ Per. But it could also be a precursory phase of a Be/X-ray binary. In that case the sdO star would represent a progenitor of a supernova.

3.4 Phase-locked emission variability

On the basis of the of 28.192 d period the short-term variability of 59 Cyg was investigated. These variations are phase-locked to the orbital period and reappear at the same phase after each orbital cycle. For the analysis dynamical spectra were calculated for several emission lines of different ions and for blended lines. The single line profiles were sorted into 20 phase bins. Four types of phase-locked variability can be distinguished:

- Single-peaked emission
- V/R variability
- Knotty absorption structure
- Variability of the equivalent width

These variations will be described in the following subsections and an explanation will be given in Section 4.

Table III. Orbital and stellar parameters of 59 Cyg. Comparison of values given in the literature and determined in this study. [1]: The value was derived by Harmanec et al. (2000) from the time of periastron passage, T_0, as given by Rivinius and Štefl (2000).

Parameters	Rivinius and Štefl (2000)	Harmanec et al. (2002)	This study
Orbital period, $\mathcal{P}$	28.1702 ±0.0014 d	28.1971 ±0.0038 d	28.192 ±0.004 d
Time of minimal RV, $T_{\min.\,\mathrm{RV}}$	50013.1 [1]	50013.31 ±0.62	–
Time of periastron passage, T_0	50018.9 ±2.5	–	51035.37
Eccentricity, e	0.20 ±0.08	0 fixed	0.11 ±0.005
Periastron length, Φ	271 ±35°	–	293±3°
Velocity amplitude of prim., K_1	26.1 km/s	13.0 ±1.0 km/s	24.77 km/s
Velocity amplitude of sec., K_2	–	$60 \leq K_2 \leq 150$ km/s	120.13 km/s
System velocity, v_0	–	−16.49 ±0.76 km/s	−0.92 km/s
Inclination, i	–	$45° < i < 90°$	$60° < i < 80°$
Mass of primary, M_1	–	10.78 $M_\odot$	$7.57 < M_1 < 11.14$ $M_\odot$
Mass of secondary, M_2	–	$1 < M_2 < 2$ $M_\odot$	$1.56 < M_2 < 2.3$ $M_\odot$
Semi-major axes of prim., a_1	–	–	$13.92 < a_1 < 15.83$ $R_\odot$
Semi-major axes of sec., a_2	–	–	$67.53 < a_2 < 76.79$ $R_\odot$
Separation of components, a	–	≈ 90 $R_\odot$	$81.46 < a < 92.63$ $R_\odot$

3.4.1 Single-peaked emission

In the dynamical spectrum of HeI 6678 the single-peaked emission is very well visible (Fig. 2). It varies in strength over an orbital cycle. Between orbital phases 0.55 and 0.9 it is most pronounced in the blue line wing and between phases 0.05 and 0.35 in the red one. The feature moves in anti-phase to the underlying absorption core of the helium line which represents the motion of the Be primary. Hence, it must be linked to the motion of the companion. It is confined to a velocity range of about ±200 km/s. In this range also the double-peaked disc emission appears which is visible in the spectra of single Be stars, too. Since this emission feature forms in the entire disc surrounding the Be star, it follows the motion of the underlying photospheric absorption profile and, thus, the Be primary. The blue peak of the double-peaked emission is very well visible between phases 0.0 and 0.5 at about −200 km/s (Fig. 2). The red pea k is less pronounced and best visible between phases 0.5 and 1.0 at roughly +200 km/s. The finding that single- and double-peaked emission appear in the same velocity range is a hint that the single-peaked emission is also formed in the disc of the Be star.

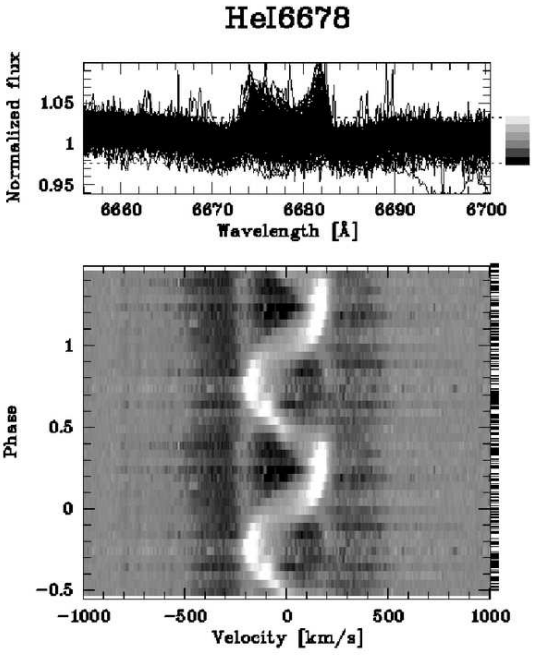

Figure 2: Dynamical spectrum of HeI 6678. The single-peaked emission appears in a velocity range of about ±200 km/s and is very well pronounced. It moves in anti-phase to the underlying absorption core and to the much weaker double-peaked emission which is also visible in the spectra of single Be stars.

3.4.2 V/R variability

The V/R variability of the emission is best visible in the line profiles of HeI 6678. It becomes obviously when a series of single spectra are plotted over an entire orbital cycle (Fig. 3). Shortly after orbital phase 0.0 an emission feature appears in the red wing of the spectral line at a velocity of roughly +100 km/s. Its strength increases, while it is moving further to the red part of the line profile. A well defined, strongly pronounced emission peak is visible between phases 0.2 and 0.3 at about +200 km/s. Here the red component of the double-peaked disc emission is located, too. Around phase 0.35 the emission feature weakens again and becomes broader. It starts to move a little bit back to the blue part of the spectral line and vanishes around phase 0.45.

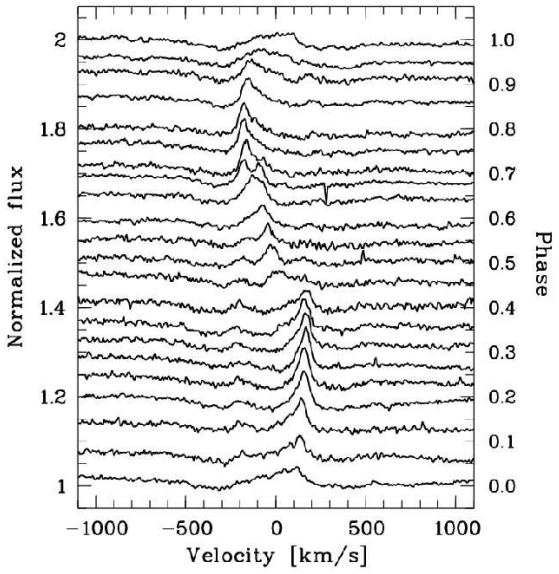

Figure 3: Observed line profiles of HeI 6678, plotted for an entire orbital cycle. The V/R variability of the emission is well visible.

At orbital phase 0.4, just before the emission feature has totally disappeared in the red part of the line wing, a second peak starts to form in the central part of the profile. It gets stronger and broader and moves further to the blue wing. Around phase 0.65 it is very broad, strongly pronounced and shows a characteristic double-peaked structure, the so-called satellite absorption. This feature is visible in the spectra of many known Be binaries and seems to be characteristic for these systems. Around phase 0.7 the red peak of this feature decreases, while the blue peak becomes more pronounced. A well defined, less pronounced, and narrow single-peaked emission is visible between phases 0.75 and 0.85 at roughly −200 km/s. There, also the blue component of the double-peaked disc emission is located. Around phase 0.9 the emission peak becomes weaker. It begins to disappear again around phase 0.95.

3.4.3 Knotty absorption structure

The orbital motion of the Be primary is clearly visible in the dynamical spectra of the photospheric absorption lines (Fig. 1, left). The line profiles are shifted periodically throughout the orbital cycle. The inner parts of the absorption wings close to the line centres, however, seem to behave not always homogeneously. During some orbital phases the inner blue wings move towards the blue part of the spectral lines, while the inner red wings seem to move redwards and, hence, to the opposite direction. The resulting "knotty structure" of the line centres is well pronounced in HeI 4471 (Fig. 1, left).

In dynamical spectra of emission lines like HeI 5876, Hβ, and P17 where the single-peaked emission is less pronounced in a velocity range of about ±100 km/s, a knotty structure is also visible quite well in the line centres. It resembles the one observed in the absorption lines. The structure does not appear in emission lines like HeI 6678 or Hα with strong central emission.

3.4.4 Variability of the equivalent widths

Equivalent widths were derived for the strong emission lines Hα and Hβ and for HeI 6678. The equivalent widths and, therefore, the emission strengths of Hα and Hβ are clearly linked to the orbital cycle (Fig. 4). Since these lines are dominated by emission, their equivalent widths are negative by definition. For convenience, the measured values were multiplicated by a factor of −1 and plotted for two orbital cycles. Due to long-term variations of the emission strength and, hence, of the equivalent widths only data are shown which were derived from spectra taken in 2000. During that year the emission was quite strong resulting in a well pronounced feature. For HeI 6678, a variability is not detectable unambiguously.

The equivalent widths of Hα and Hβ show maximum strength around phase 0.0 and 1.0, respectively. Then, the companion is located in front of the Be primary. Towards phase 0.5, when the secondary moves in opposite direction to an observer and, hence, behind the Be star, the equivalent widths decrease. Minimum strength is reached around phase 0.4. After orbital phase 0.4 the equivalent widths increase again till they attain maximal strength around phase 1.0 or 0.0, respectively. During these orbital phases the sdO companion moves towards an observer in front of the primary component.

4 Sector model

The different types of short-term, phase-locked variability observed in the spectrum of 59 Cyg and described in sections 3.4.1 to 3.4.4 can be entirely explained by one and the same process. According to the sector model of Štefl et al. (2000) a sector of the circumstellar disc of a Be star facing a hot, low-mass companion is partially photo-ionized by the UV radiation of the secondary, a sdO star or a hot white dwarf. This sector gives rise to extra emission. Since this emission is formed only in a part of the Be disc, it is single-peaked and linked to the motion of the companion. Therefore, it moves in anti-phase to the radial velocity curve of the Be primary. This extra emission causes phase locked variability and is observationally visible as a single-peaked emission component and as short-term V/R variations.

Using the sector model, Hummel and Štefl (2001)

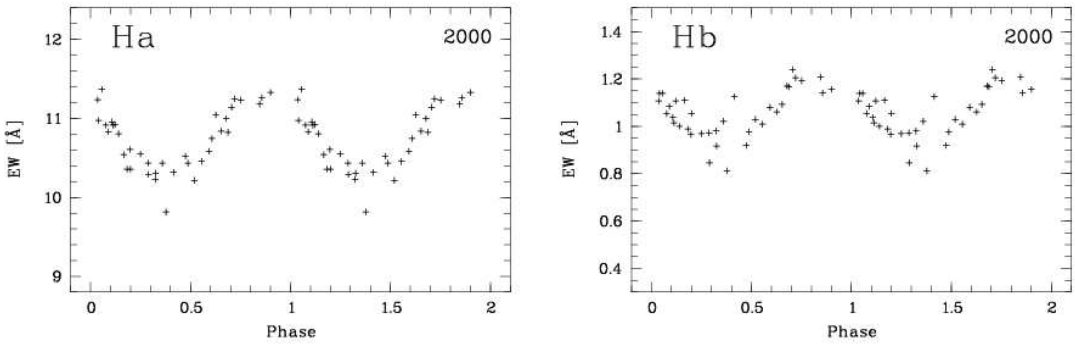

Figure 4: Variability of the equivalent widths of Hα and Hβ in the year 2000. For more convenience the data were multiplicated by a factor of -1 and plotted for two orbital cycles. The connection of the emission strength with the orbital cycle is well visible.

successfully reproduced the phase-locked variability of the HeI 6678 and HeI 5876 emission of ϕ Per which resembles the single-peaked emission observed in the spectrum of 59 Cyg. In contrast to earlier models, the sector model is the first quantitative one. Only a small number of physical components, i.e. the Be primary, the hot secondary, and the disc surrounding the Be star, are required. Furthermore, it explains the origin of the observed emission variability within the scope of only one physical component which is represented by the disc of the Be star.

4.1 Model-geometry

The geometry assumed for the Be primary of 59 Cyg is shown in Figure 5 for orbital phases 0.0, 0.25, 0.5, and 0.75. Phase 0.0 corresponds to zero radial velocity of both binary components when the secondary and, thus, the photo-ionized disc sector are in front of the Be star. The circumstellar disc of the Be primary is co-planar to the orbital plane of the binary. Additionally, the profiles of the HeI 6678 line of 59 Cyg observed at the given orbital phases are shown. Strength and appearance of the extra emission are determined by the geometrical position of the disc sector.

4.2 Extra emission

At phase 0.25 and 0.75 the extra emission appears as a strong and sharp emission peak. It is maximally redshifted around phase 0.25 and maximally blueshifted around phase 0.75. At phase 0.5 the extra emission is visible as a small, but well defined peak in the line centre. A broad, nearly featureless emission dominates the line centre at phase 0.0. The very small blue peak of the double-peaked emission from the entire Be disc is also visible at about -200 km/s at phase 0.25 and 0.5. At phase 0.5 even the red peak is detectable at roughly +200 km/s. The single-peaked emission is confined to the velocity range given by the peak separation of the double-peaked emission. The feature can be interpreted as V/R variability, too.

Also the knotty absorption structure visible in dynamical spectra of absorption and some emission lines, which could be misinterpreted as an effect of incorrect phase-binning due to a wrong orbital period, can be explained by this model. Figure 6 shows a comparison of the dynamical spectra of HeI 6678 (left) and HeI 5876 (right). It demonstrates that the knotty absorption features cannot be explained without taking into account the extra emission from the disc sector. The cut values for the line intensities has been chosen in a way that the double-peaked disc emission and the single-peaked extra emission are well visible.

In HeI 6678 the single-peaked emission is strongly pronounced and clearly visible throughout the line profile. Thus, the spectral line does not show a knotty absorption structure. In HeI 5876, however, the extra emission is well detectable in the line wings only where the double-peaked disc emission appears, too. It is not visible in the central part of the line profile. Hence, it follows that the knotty structure results due to a superposition of the single-peaked emission, the double-peaked emission and the absorption profile of a spectral line when the extra emission is less pronounced in the inner region of the line centre. That also means that a spectral line must have a contribution of the extra emission if its line centre shows such a knotty absorption feature. Thus, the knotty structure is an indicator for emission from a photo-ionized disc sector in a Be binary even if the emission is too weak to be traced directly.

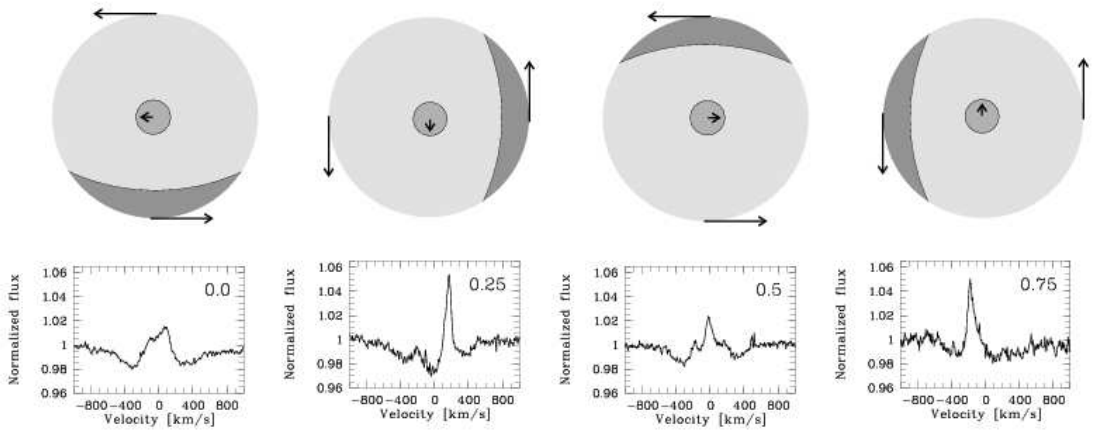

Figure 5: Geometry of the Be primary of 59 Cyg according to the sector model, viewed from above the orbital plane, and observed HeI 6678 emission for orbital phases 0.0, 0.25, 0.5, and 0.75 (from left to right). Grey centre: Be primary; Light-grey: Circumstellar disc of the Be star; Dark-grey: Disc sector facing the secondary, photo-ionized by the UV continuum radiation of the sdO star. The long arrows mark the sense of rotation of the disc. The short arrows mark the direction of movement of the Be star.

4.3 Projected sector area

The variability of the equivalent widths of the optically thick emission lines Hα and Hβ which clearly follows the motion of the secondary can be explained qualitatively by the photo-ionized disc sector. Around phases 0.0 and 0.5 the sector is directly in front or behind the Be star, respectively. Since the binary system is visible at an inclination larger than 60 ^{o} and lower than 80 ^{o}, the plane and the edge of the Be disc are well visible. Around phase 0.0 the projected area of the disc sector in direction to an observer, including plane and edge of the disc, reaches its maximum. Therefore, a maximal amount of variable emission, originating in the photo-ionized sector, is visible. Around phase 0.5 the projected area of the disc sector is minimal, since only the surface of the sector is visible, but not the edge. Therefore, the amount of variable emission, detectable for an observer, is expected to be minimal.

As shown in Figure 4, this expectation is not fully matched by the observations. Instead of showing a minimum at phase 0.5, the equivalent widths are minimal at phase 0.4. Then, they start to increase again. This behaviour is explicable by the periastron passage which takes place at phase 0.57. When the secondary moves towards the Be star, it comes closer to the disc and illuminates a larger area. In addition, it is expected that also deeper layers will be photo-ionized. This is expected to result in enhanced extra emission around periastron, which is exactly what is observed. Therefore, the properties of the periodic variability of the equivalent widths confirm an eccentric orbit for 59 Cyg.

5 Characteristic features

The analysis of the Be binary 59 Cyg revealed spectral features which are fully explained and predicted by the sector model for Be binaries with a sdO star or a hot white dwarf component described by Štefl et al. (2000) and Hummel and Štefl (2001). These features can, therefore, be regarded as characteristic for this kind of double stars and can be taken as indicators for the identification of further evolved Be binaries with hot, compact companions.

Except of the variability of the equivalent widths of optically thick lines all of the described features including a HeII 4686 line were observed in the spectrum of ϕ Per, too (Poeckert 1981; Štefl et al. 2000). Since ϕ Per has a higher inclination angle compared to 59 Cyg, it additionally shows regular short-lived shell events. Shell lines appear when the photo-ionized disc sector is located in front of the Be star in the line of sight of an observer. They were also successfully modelled by Hummel and Štefl (2001).

6 Conclusions

59 Cyg was confirmed to be a Be + sdO binary with an orbital period of 28.192 $\pm$0.004 d. The companion was directly proved by a HeII 4686 absorption. Radial velocity curves were determined for both binary components. Orbital and stellar parameters were derived. The mass of the secondary lies most likely between 1.56 and 2.3 $M_{\odot}$. According to evolutionary models for Be binaries, 59 Cyg seems to represent a ϕ Per like system in an earlier stage. But it can also be the progenitor of a Be + WD or Be/X-ray binary.

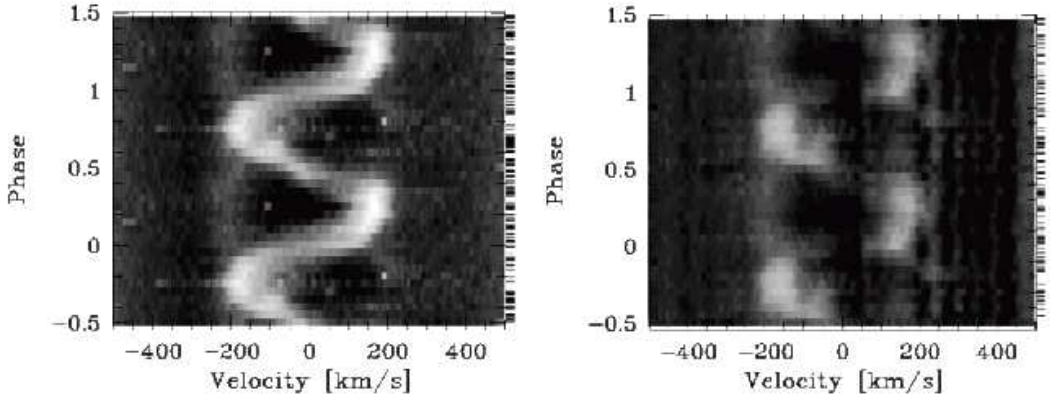

Figure 6: Central parts of the emission lines HeI 6678 (left) and HeI 5876 (right). The cut values for the line intensities are chosen in a way that the course of both emission components, the phase-locked single-peaked emission and the double-peaked disc emission, becomes clearly visible. In HeI 5876, where the single-peaked emission is less pronounced, a knotty absorption structure is visible. In contrast, it does not appear in HeI 6678.

The short-term, phase-linked variability of 59 Cyg is entirely explained by the sector model of Štefl et al. (2000) and Hummel and Štefl (2001). An evolved Be binary with a hot, low-mass companion, a sdO star or a hot white dwarf, is assumed. The part of the Be disc which phases the secondary is partly photo-ionized by the UV radiation of the hot companion. This disc sector gives rise to a single-peaked extra emission component.

The spectral features caused by the single-peaked emission or the photo-ionized sector itself are generally predicted by the sector model and are, hence, characteristic for Be + sdO and Be + WD binaries. Including the HeII 4686 line these are:

- HeII 4686 emission or absorption
- Single-peaked emission
- Short-term V/R variability of the emission
- Knotty absorption structure
- Variability of the equivalent widths
- Periodic, short-lived shell phases

These features are observed in the spectra of 59 Cyg and/or ϕ Per. They can be taken as indicators to identify other Be binaries with sdO or white dwarf companions more easily.

Evolved Be binaries are difficult to detect due to the low-mass secondary. 59 Cyg showed that even a very well studied Be star was confirmed to be a double star only in the recent years. Thus, it is most likely that a fraction of the Be stars indeed formed by close binary evolution. They are still not observed yet.

Acknowledgement

We thank the Stellar Department of the Astronomical Institute in Ondřejov, Czech Republic, for the possibility to carry out a long-term monitoring campaign of Be and Bn stars with the HEROS spectrograph at the 2 m telescope of the observatory and for the good co-operation.

References

Harmanec P., Božić H., Percy J. R., Yang S., et al.: 2002, A&A 387, 580
Hummel W., Štefl S.: 2001, A&A 368, 471
Hutchings J. B., Stoeckley T. R.: 1977, PASP 89, 19
Jaschek M., Slettebak A., Jaschek C.: 1981, BeSN 4, 9
Kaufer A.: 1996, PhD thesis, Ruperto-Carola University of Heidelberg, Germany.
Kaufer A.: 1998, Rev. Mod. Astron. 11, 177
Maeder A., Grebel E. K., Mermilliod J.-C.: 1999, A&A 364, 459
Mandel H.: 1988, PhD thesis, Ruperto-Carola University of Heidelberg, Germany
Mandel H.: 1994, in: The Impact of Long-Term Monitoring on Variable Star Research, ed. C. Sterken, M. de Groot, NATO ASI Series C 436, Kluwer Acad. Publ., 303
Owocki S. P.: 2004, in: Stellar Rotation. IAU Symp. 215, ed. A. Maeder & P. Eenens, p. 515
Poeckert R.: 1981, PASP 93, 297
Pols O. R., Coté J., Waters L. B. F. M., Heise J.: 1991, A&A 241, 419
Raguzova N. V.: 2001, A&A 367, 848
Scargle J. D.: 1982, ApJ 263, 835
Schwarzenberg-Czerny A.: 1989, MNRAS 241, 153
Slettebak A.: 1982, ApJS 50, 55
Stahl O., Kaufer A., Wolf B., et al.: 1995, J. Astron. Data 1, 3 (on CD-ROM).
Štefl S., Hummel W., Rivinius T.: 2000, A&A 358, 208
Van Bever J., Vanbeveren D.: 1997, A&A 322, 116
Vanbeveren D., van Rensbergen W., de Loore C.: 1998, The brightest Binaries, Kluwer Acad. Publ.